Numerical Study of Single Impinging Jets Through a Crossflow

J. M. M. Barata* and D. F. G. Durão†
Instituto Superior Técnico, Lisbon, Portugal
and
J. J. McGuirk‡
Imperial College of Science and Technology, London, England

This paper describes the application of three-dimensional finite-difference calculation procedures to the problem of a jet impinging on a flat plate through the influence of a confined crossflow. One procedure uses the hybrid central/upwind difference scheme, and the other uses a quadratic upstream weighted difference scheme (QUICK) to calculate the convection terms. The standard two-equation "$k-\epsilon$" turbulence model is used to calculate the distribution of the Reynolds stresses. The difficulty of assessing turbulence model performance in these complex flows due to the intrusion of numerical diffusion errors is demonstrated by comparing the calculations on both coarse and fine meshes and by improving the accuracy of the convection terms discretization using the higher-order QUICK method. The ability of the model calculations to simulate both the mean and the turbulence fields is examined, particularly in the vicinity of the stagnation point. The results show the advantages of QUICK differencing scheme over the hybrid treatment, since the same level of numerical accuracy requires far less CPU time and computer memory when the QUICK scheme is used. The calculations reveal the existence of large regions of low pressure, associated with an upstream recirculating flow region due to the interaction between the upstream wall jet and the crossflow, which may produce a substantial lift loss for a VSTOL aircraft.

Nomenclature

$A^{\phi}_{P,N,S,W,E,L,R}$	= coefficients of the finite-difference equation
C_1, C_2, C_μ	= constants in turbulence model
D	= diameter of the jet
H	= height of the crossflow channel
k	= turbulence kinetic energy
Pe	= cell face Peclet number
Re	= Reynolds number
S_ϕ	= source of dependent variable ϕ
S^{ϕ}_P, S^{ϕ}_U	= components of linearized source term
U	= horizontal velocity, $= \bar{U} + u'$
V	= vertical velocity, $= \bar{V} + v'$
X	= horizontal coordinate (positive in the direction of crossflow)
Y	= vertical coordinate (positive in the direction of jet flow)
Z	= transverse coordinate (positive on right side of crossflow duct looking upstream)
δ_{ij}	= Kronecker delta
ϵ	= dissipation rate of k
Γ_ϕ	= transport coefficient of dependent variable
ϕ	= dependent variable
$\phi_{P,N,S,W,E,L,R}$	= values of ϕ at nodes P,N,S,W,E,L,R
$\sigma_{k,\epsilon}$	= Prandtl/Schmidt numbers for k and ϵ
ν	= kinematic viscosity

Subscripts

j	= jet-exit value
0	= crossflow value

I. Introduction

THE flow of a single jet issuing into a crossflow is a basic flow configuration with many practical applications, such as the dispersal of pollutants from chimney stacks, discrete-hole film cooling of turbine blades, the injection of air into the dilution zone of a gas-turbine combustor, the discharge of waste liquids into rivers, and the flowfield beneath a short take-off/vertical landing (VSTOL) aircraft close to the ground. In this latter application, the lift jets interact strongly with the ground plane, resulting in lift losses, enhanced entrainment close to the ground (suckdown), in engine thrust losses following re-ingestion of the exhaust gases, and in instabilities caused by fountain impingement on the aircraft underside.

The study of a single jet in crossflow that subsequently undergoes impingement on a ground plane provides a basis to understanding the essential dynamics of these complex practical flowfields. The present paper describes a computational study of the flow produced by a single round jet discharged through the upper wall of a rectangular water channel of large cross section (0.50×0.10 m) at right angles to the channel flow, as shown schematically in Fig. 1. The objective of this work is the development and validation of a computational method based on the solution of time-averaged Navier-Stokes equations and the $k-\epsilon$ turbulence model. The method is then used to study phenomena that affect vertical short take off landing (VSTOL) aircraft performance and safety: the formation of a vortex that wraps around the impingement point and the existence of low pressures in the neighborhood of the jet.

Experimental and theoretical studies have been carried out on these kind of flows with different motivations, depending on the jet-to-crossflow velocity ratio and geometries. Much of the published work is centered on the unconfined problem and on large ratios between the height of the jet exit above the ground plane and the jet diameter (H/D), and on such low-

Presented as Paper 89-0449 at the AIAA 27th Aerospace Sciences Meeting, Reno, NV, Jan. 9-12, 1989; received Oct. 24, 1988; revision received April 6, 1989.

*Lecturer, Department of Mechanical Engineering.
†Professor, Department of Mechanical Engineering; Dean of Instituto Superior Técnico.
‡Lecturer, Department of Mechanical Engineering.

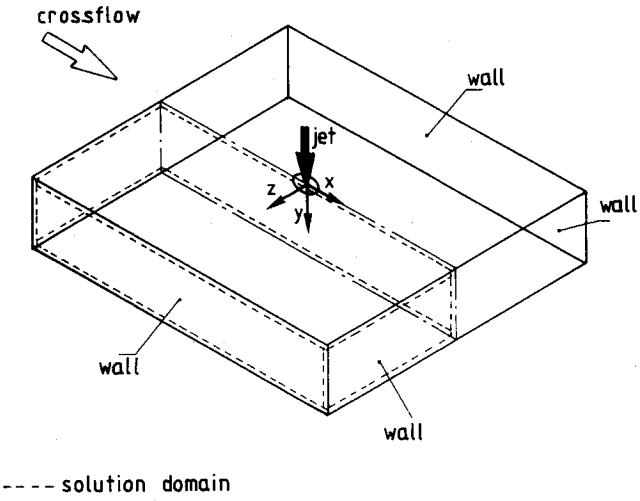

Fig. 1 Flow configuration.

velocity ratios ($V_j/U_0 < 10$) as to be of little use in the present context. The theoretical work on these flows has mainly involved the application of integral methods. Keffer and Baines[1] and Adler and Baron[2] predicted jet trajectories using integral methods that need as input the specification of an entrainment function. In the former study, the jet cross section is assumed to be elliptical or circular, but in the latter, the need of prescribing the jet cross section was eliminated. Patankar et al.[3] used a finite-difference method with a two-equation model of turbulence and obtained good agreement with the experiments of Refs. 1 and 4. Rodi and Srivatsa[5] presented a locally elliptic finite-difference procedure and showed total pressure distributions that agree with the experiments for a very low jet-to-crossflow velocity ratio (0.1), but the agreement got worse as the velocity ratio increased. Baker et al.[6] used a three-dimensional finite-element algorithm to study the flow produced by a jet issued perpendicular to a flat plate into a crossflow at a higher velocity ratio $V_j/U_0 = 10$, but presented mean velocity distributions only in the initial jet region. If attention is restricted to the high-velocity ratios/small impingement height combination, then no relevant numerical studies may be found. Jones and McGuirk[7] did report some calculations of impinging jets in confined crossflow, but little attention was given to the strongly impinging case. Although a two-equation $k-\epsilon$ model was employed in these calculations, the use of first-order upwind differencing and very coarse meshes made any statements on turbulence model accuracy impossible. This question of false diffusion in three-dimensional jets-in-crossflow calculations has been addressed by Demuren,[8] who found it necessary to adopt higher-order discretization schemes for the convection terms in order to obtain numerically accurate solutions. Childs and Nixon[9] presented calculations relevant to the VSTOL problem using the $k-\epsilon$ model and confirmed the gross features of the flow, but little comparison was given against experimental data to enable a quantitative judgment of the calculations. Barata et al.[10] have also reported some numerical calculations for a jet configuration relevant to VSTOL obtained with the hybrid central/upwind differencing scheme, providing a preliminary examination of the $k-\epsilon$ turbulence model based on their detailed measurements, and also have shown some qualitative results that indicate the need of a higher-order method. The calculations presented in this paper follow those reported by Barata et al.[10] and show the improvements that could be achieved by using the higher-order scheme QUICK of Leonard.[11]

The next section gives the details of the mathematical model. Section III presents a quantitative comparison of numerical results with the measurements of Barata et al.[10] in order to evaluate the predictive capabilities of the solution procedures, which is followed by an analysis of the pressure field and the formation of the ground vortex. The final section summarizes the main findings and conclusions of this work.

II. Mathematical Model

A. Governing Differential Equations

The time-averaged partial differential equations governing the steady, uniform-density isothermal three-dimensional flow may be written in Cartesian coordinates as

$$\rho \bar{U}_j \frac{\partial \bar{U}_i}{\partial X_j} = -\frac{\partial \bar{P}}{\partial X_i} + \frac{\partial}{\partial X_j}\left(\mu \frac{\partial \bar{U}_i}{\partial X_j} - \rho \overline{u_i' u_j'}\right) \tag{1}$$

and the continuity equation as

$$\rho \frac{\partial \bar{U}_i}{\partial X_i} = 0 \tag{2}$$

where the overbars represent averaged quantities. The turbulent diffusion fluxes are approximated with the high Reynolds number version of the two-equation $k-\epsilon$ model described in detail by Launder and Spalding.[12] The Reynolds stresses may be expressed as

$$\overline{u_i' u_j'} = -\nu_T\left(\frac{\partial \bar{U}_i}{\partial X_j} + \frac{\partial \bar{U}_j}{\partial X_i}\right) + \frac{2}{3} k \delta_{ij} \tag{3}$$

where ν_T is the turbulence kinematic viscosity, which is derived from the turbulence model and expressed by

$$\nu_T = C_\mu k^2/\epsilon \tag{4}$$

The values for k and ϵ are obtained by solving the following transport equations:

$$\bar{U}_j \frac{\partial k}{\partial X_j} = \frac{\partial}{\partial X_j}\left(\frac{\nu_T}{\sigma_k}\frac{\partial k}{\partial X_j}\right) - \overline{u_i' u_j'}\frac{\partial \bar{U}_i}{\partial X_j} - \epsilon \tag{5}$$

$$\bar{U}_j \frac{\partial \epsilon}{\partial X_j} = \frac{\partial}{\partial X_j}\left(\frac{\nu_T}{\sigma_\epsilon}\frac{\partial \epsilon}{\partial X_j}\right) - C_1 \frac{\epsilon}{k}\overline{u_i' u_j'}\frac{\partial \bar{U}_i}{\partial X_j} - C_2 \frac{\epsilon^2}{k} \tag{6}$$

The turbulence model constants that are used are those indicated by Launder and Spalding[12]:

C_μ	C_1	C_2	σ_k	σ_ϵ
0.09	1.44	1.92	1.0	1.3

The governing equations constitute a set of coupled partial differential equations that can be written in the general form as

$$\frac{\partial U\phi}{\partial X} + \frac{\partial V\phi}{\partial Y} + \frac{\partial W\phi}{\partial Z} = \frac{\partial}{\partial X}\left(\Gamma_\phi \frac{\partial \phi}{\partial X}\right) + \frac{\partial}{\partial Y}\left(\Gamma_\phi \frac{\partial \phi}{\partial Y}\right) + \frac{\partial}{\partial Z}\left(\Gamma_\phi \frac{\partial \phi}{\partial Z}\right) + S_\phi \tag{7}$$

where ϕ may stand for any of the velocities, turbulent kinetic energy, or dissipation, and Γ_ϕ and S_ϕ take on different values for each particular ϕ.

B. Finite-Difference Equations

The solution of the governing equations were obtained using a finite-difference method that used discretized algebraic equations deduced from the exact differential equations that they represent. This discretization involves the integration of the transport equation (7) over an elementary control volume surrounding a central node with a scalar value ϕ_P (e.g., Leon-

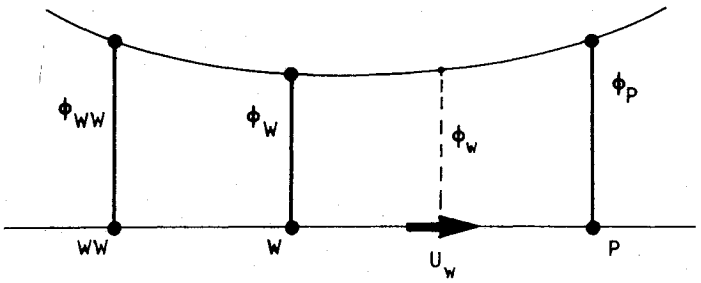

Fig. 2 Nodal configuration for the west face of a control volume.

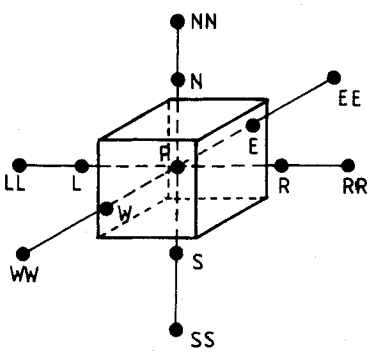

Fig. 3 Nodal configuration for a control volume surrounding a central node *P*.

ard et al.[13]), and as far as the convection terms are concerned, it needs the spatial average value of ϕ at each cell face. The hybrid scheme uses central differencing in obtaining those values when $Pe < 2$ and upwind differencing for $Pe \geq 2$. In the latter case, false diffusion is introduced into the finite-difference equation (e.g., Leonard[11]). Erroneous solution may then be obtained in regions of the flow with velocity vectors inclined to the numerical grid lines and large diffusive transport normal to flow direction if fine grids are not used, and limit calculation of complex flows. The QUICK scheme proposed by Leonard[11] is free from artificial diffusion and gives more accurate solutions with grid spacing much larger than that required by the hybrid scheme. This is achieved by utilizing quadratic upstream-weighted interpolation to calculate the cell face values for each control volume. Figure 2 shows the *west* face of a control volume surrounding a central node with a value ϕ_P. For this face, using a uniform grid for simplicity, the value of ϕ is expressed by

$$\phi_w = \tfrac{1}{2}(\phi_P + \phi_W) - \tfrac{1}{8}(\phi_P + \phi_W + \phi_{WW}) \tag{8}$$

if the convective velocity component U_W is assumed to have the direction shown in Fig. 2. If U_W were negative, then ϕ_{WW} would be involved rather than ϕ_E. The first term in Eq. (8) is the central difference formula, and the second is the important stabilizing upstream-weighted normal curvature contribution. Expressing the values of ϕ at each cell face with the appropriate interpolation formula and writing gradients also in terms of node values, the finite-difference equation corresponding to Eq. (7) may be written in the general form

$$A_P^\phi \phi_P = \sum A_i^\phi \phi_i + S_U^\phi \tag{9}$$

where

$$A_P^\phi = \sum A_i^\phi - S_P^\phi \tag{10}$$

Here, the summation occurs over the 12 nodes neighboring P (see Fig. 3). The set of equations for the complete field is solved by the method usually used with hybrid scheme formulation (see Gosman and Pun[14]), but when using QUICK, the A_i^ϕ coefficients may become negative and stable solutions cannot be obtained. Han et al.[15] inserted the curvature term of Eq. (8) into the source term and used only the central-difference contribution to the convective term. This procedure revealed the instabilities of the central differencing scheme, and convergence could only be obtained by using a false transient technique, although rather slowly. To avoid the false transient terms and obtain faster convergence, these authors tested different decompositions of the quadratic interpolation expressions using a part of the curvature contribution to evaluate the convection term. These expressions had to be evaluated using the values of ϕ calculated at the previous iteration cycle; otherwise, convergence was very difficult. Moreover, the false-transient terms could not be avoided when calculating turbulent flows, and the rate of convergence was deteriorated. In the present work, diagonal dominance of the coefficient matrix is ensured and enhanced by rearranging the difference equation for the cells where the coefficients A_i^ϕ become negative. This rearrangement consists in subtracting $A_i^\phi \phi_P$ from both sides of Eq. (9), eliminating the negative contribution of A_i^ϕ and simultaneously enhancing the diagonal dominance of the coefficient matrix. The source term S_U^ϕ becomes

$$S_U^\phi = S_U^\phi - A_i^\phi \phi_P' \tag{11}$$

where ϕ_P' is the latest available value of ϕ at node P. Rhode et al.[16] recently used a similar practice, but have employed the hybrid scheme in the k and ϵ equations following the suggestions of Leschziner and Rodi.[17] The reason given by these authors was that in high shear zones, the k and ϵ are source- and sink-dominated, but no comparison between the two procedures was given. Han et al.[15] present the effect of grid refinement and use of QUICK for k and ϵ on the distribution of turbulent viscosity in a driven cavity, and found that the calculated level of ν_T is particularly sensitive to numerical diffusion. Therefore, at the present work, the QUICK scheme is used in calculating all the variables.

C. Solution Procedure

The solution procedure is based on the SIMPLE algorithm widely used and reported in the literature (e.g., Patankar and Spalding[18]). It uses the staggered grid arrangement and a guess and correct procedure to solve the problem of obtaining a pressure field such that the solution of the momentum equations satisfies continuity.

D. Boundary Conditions

The computational domain has six boundaries where dependent values are specified: an inlet and outlet plane, a symmetry plane, and three solid walls at the top, bottom, and side of the channel. The sensitivity of the solutions to the location of the inlet and outlet planes was investigated, and their final position is sufficiently far away from the jet so that the influence on the computed results is negligible. At the inlet boundary, uniform profiles of all dependent variables are specified from the experimental results. At the outflow boundary, the gradients of dependent variables in the axial direction are set to zero. On the symmetry plane, the normal velocity vanishes, and the normal derivates of the other variables are zero. At the solid surfaces, the wall function method described in detail by Launder and Spalding[12] is used to prescribe the boundary conditions for the velocity and turbulence quantities, assuming that the turbulence is in state of local equilibrium. The jet-exit boundary is represented by a right-angled polygon, and the mass flow rates and the momentum of the jet are matched to the experimental values. Preliminary tests used the exact shape of the jet exit by modifying the cell face areas where the hole boundary bisected the surface area of the adjacent finite-difference control volume, so that the specified jet velocity produces correct fluxes; the velocity distribution downstream of the jet exit was relatively insensitive to the

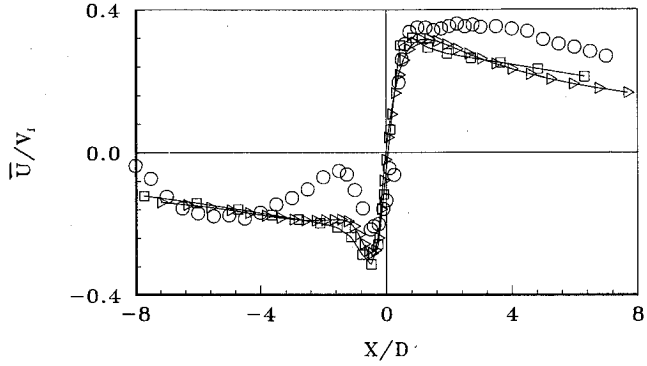

Fig. 4 Horizontal profiles of the mean horizontal velocity component $\bar{U}/V_j$ at $Y/D = 4.7$: ○, measurements[10]; □, QUICK $30 \times 17 \times 17$; ▷, QUICK $60 \times 34 \times 34$.

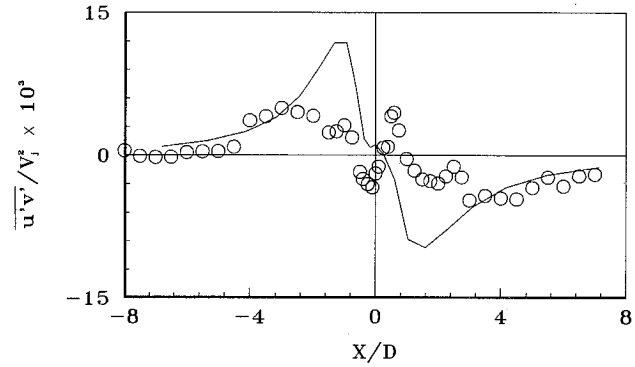

Fig. 6 Horizontal profiles of Reynolds shear stress $\overline{u'v'}/V_j^2 \times 10^3$: ○, measurements[10]; ——, QUICK ($30 \times 17 \times 17$).

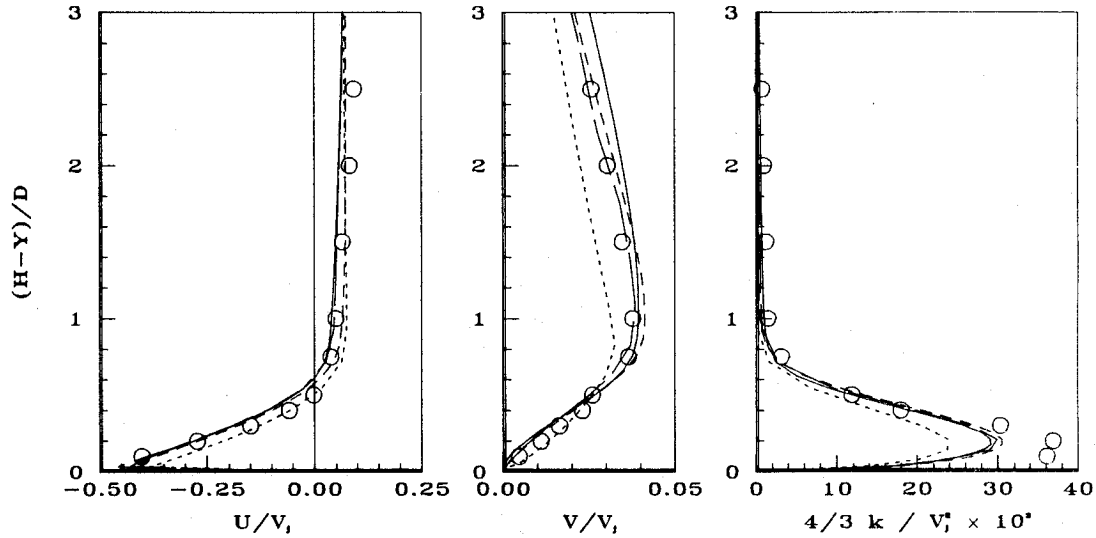

Fig. 5 Vertical profiles at $X/D = -2.5$: ○, measurements[10]; ------, hybrid ($30 \times 17 \times 17$); ----, hybrid ($60 \times 34 \times 34$); ———, QUICK ($30 \times 17 \times 17$); ——, QUICK ($60 \times 34 \times 34$).

assumed shape of the hole. The jet-exit boundary conditions are also prescribed from experiments.

III. Results and Discussion

The numerical predictions presented in this section are compared with Laser Doppler Velocimetry (LDV) measurements of Barata et al.[10] obtained on the central plane of symmetry using a single jet of 20-mm exit diameter D, 5 jet diameters above the ground plate (i.e., $H/D = 5$). The jet Reynolds number for the selected test case was $Re_j = 60{,}000$ for a jet-exit mean velocity of $V_j = 3$ m/s and a local turbulence intensity of 2% and crossflow velocity of $U_0 = 0.1$ m/s. This test case was predicted using the standard $k - \epsilon$ turbulence model together with the hybrid and QUICK schemes to evaluate the convection terms of the transport equations and meshes up to $60 \times 34 \times 34$ nodes. The grid spacing was nonuniform with grid lines clustered in the vicinity of the shear layers and impingement locations.

The predicted horizontal profiles of the horizontal velocity component $\bar{U}$ at a plane close to the impingement wall ($Y/D = 4.7$) are used to test the grid dependency of the computations. Figure 4 compares the velocity distributions with the QUICK scheme for different grid refinements. The $\bar{U}$ velocity profiles are in qualitative agreement although in the computations the values are larger than the measurements close to the impingement point at $-3 < X/D < -0.5$ and smaller for $X/D > 2$, and this is independent of numerical influences. The results for a $30 \times 17 \times 17$ grid are similar to the values generated with the $60 \times 34 \times 34$ grid and may be considered as grid-independent. In contrast, the hybrid scheme solution for a $30 \times 17 \times 17$ grid shows significant grid dependence. Figure 5 compares predicted vertical profiles obtained with the hybrid and the QUICK schemes and the coarse and the finer meshes. It shows that the use of first-order hybrid difference treatment for the convection terms can cause problems in allowing false diffusion errors to present grid independence being achieved on reasonable meshes and, thus, is masking the true performance of the turbulence model. Although the mean horizontal velocity profiles are well predicted with the two meshes and numerical schemes, the predicted mean vertical velocity and the turbulence kinetic energy profiles show clearly the effect of refining mesh and of using the higher-order QUICK method. Evidently, important savings in computing time and memory can be made with quadratic upstream interpolation, especially in three-dimensional flow. The present $30 \times 17 \times 17$ QUICK calculations required 1 MByte of memory and 3 s of CPU time per iteration on the AMDAHL machine and were obtained using 80% less computer storage and 90% less execution time than the equivalent hybrid calculations.

Figure 6 compares the measured and predicted horizontal profiles of the Reynolds shear stress for a plane close to the impingement plane ($Y/D = 4.7$) and shows not only large overpredictions of absolute values, but also significant regions where the sign is wrong. The turbulence structure in the impingement zone is obviously not simulated well by an eddy

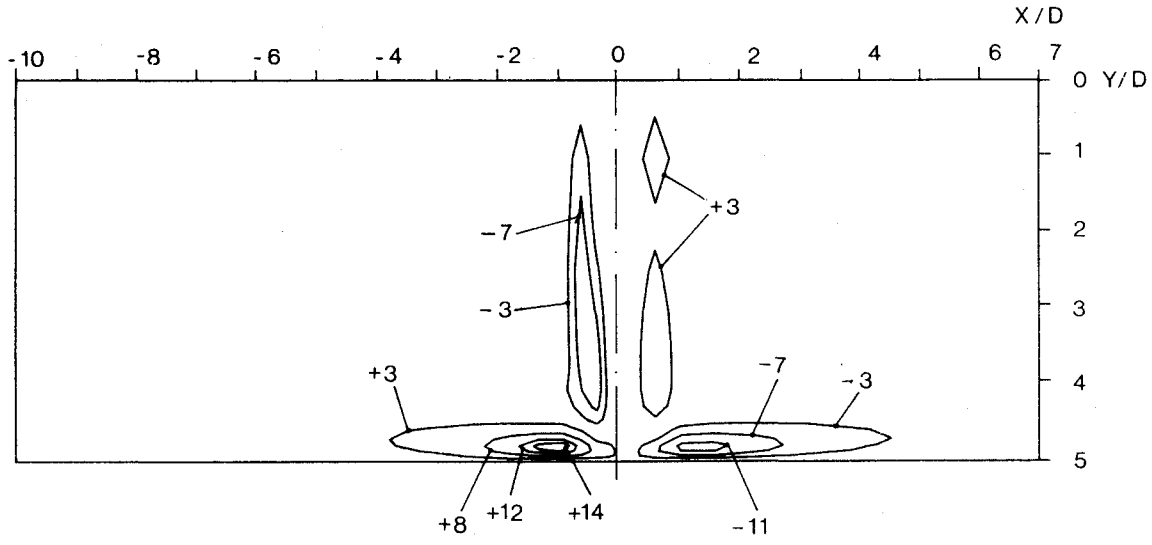

Fig. 7 Predicted contours of Reynolds shear stress $\overline{u'v'}/V_j^2 \times 10^3$ on the central symmetry plane (QUICK, 30×17×17).

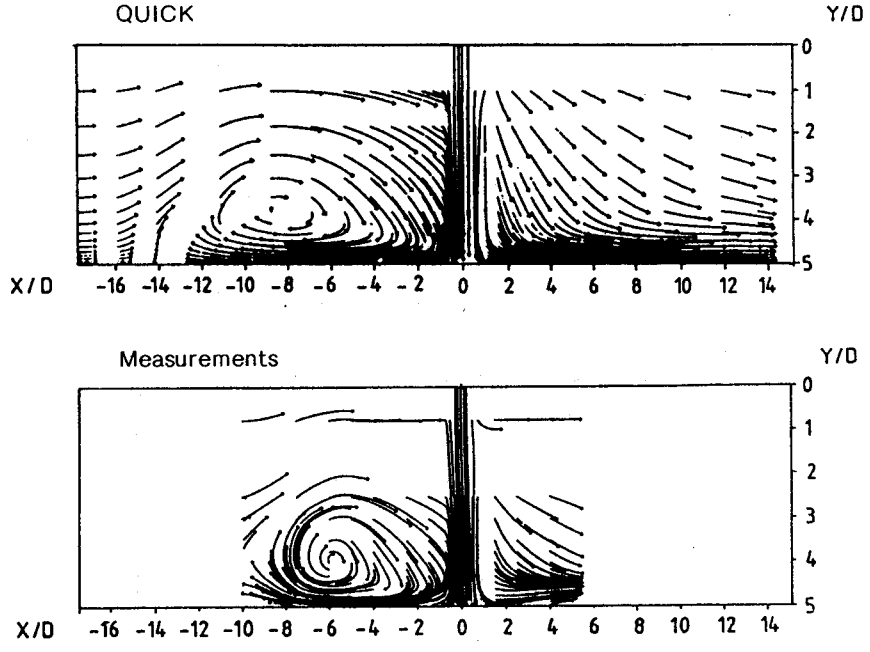

Fig. 8 Measured and predicted streak lines in the vertical plane of symmetry showing the ground vortex.

viscosity model. Away from the impingement point, the sign of the shear stress is related to the sign of the shear strain in accordance with a turbulent viscosity hypothesis, and the sign of the predicted values is correct (see Fig. 7), and its magnitude is similar to the measured values of Barata et al.[10] In spite of the failure of the turbulence model to predict the structure of the impinging zone, it should be pointed out that the corresponding effect on the simulation of the mean flow is not too significant, as shown in Fig. 5, because the flow is dominated by large pressure gradients.

Figure 8 shows particle tracks or streak lines of the predicated velocity fields on the vertical symmetry plane, which shows clearly the impinging jet with its exit located $17.5D$ downstream of the crossflow entrance and the ground vortex due to the interaction between the upstream wall jet and the crossflow. The measured mean velocities (in the region of the X-Y plane in which they are available) have been fed into the same streak-line plotting program to enable an easy comparison with the predictions. The QUICK predictions contain the flow features, although the location of the vortex seems to be predicted about $2D$ too far upstream. Figure 9 shows a streak line started in the upstream edge of the jet exit near the vertical plane of symmetry and gives the shape of the vortex, which also captures fluid from the crossflow. Figure 10 gives isobars in the impingement plane and shows a low-pressure region located under the ground vortex, and high-pressure zones upstream of the reverse flow region and downstream the impinging point (where the maximum value occurs, $p/\frac{1}{2}\rho V_j^2 = 0.84$). The low-pressure region results from the acceleration of the crossflow over the ground vortex, which has a maximum height of about 40% of the jet-exit height H. Figure 11 presents isobars on the jet-exit plane and shows a small region of high pressure in the upstream side of the jet exit, whereas the lowest values occur in the sides of the jet. Figure 12 is a three-dimensional perspective of the pressure distribution in a horizontal plane at $Y/D = 3.46$, confirming the existence of the low-pressure zone with a shape similar to the shape of the ground vortex. These results seem to indicate that the suckdown effect may be enhanced when the aircraft is operating close to the ground with a crosswind present due to the formation of the ground vortex, which is associated with lower pressures.

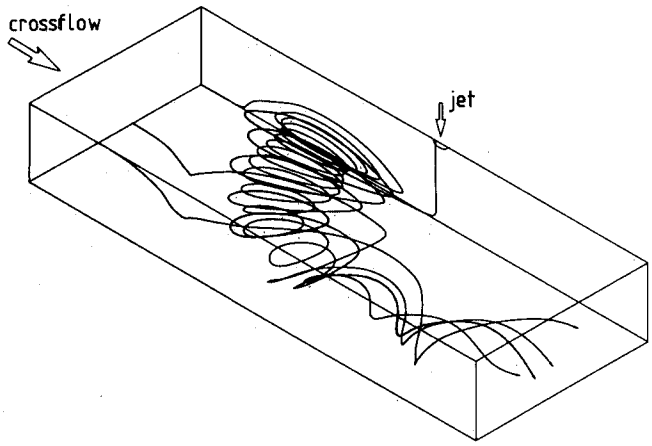

Fig. 9 Three-dimensional streak lines.

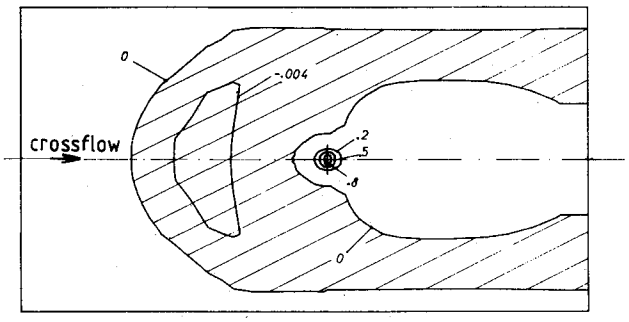

Fig. 10 Isobars on the impingement plane, $p/\frac{1}{2}\rho V_j^2$.

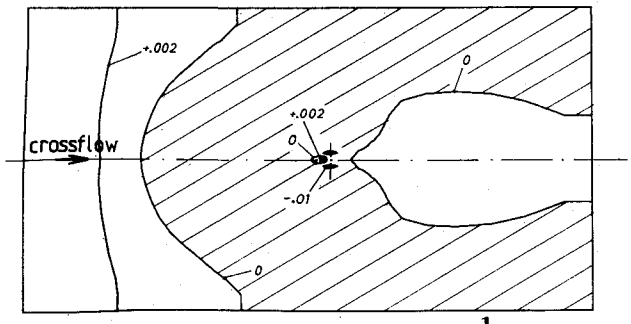

Fig. 11 Isobars on the jet-exit plane, $p/\frac{1}{2}\rho V_j^2$.

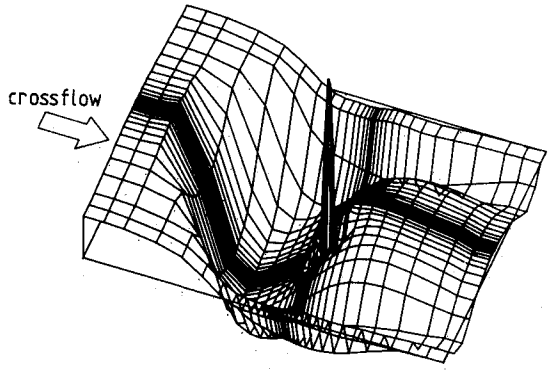

Fig. 12 Three-dimensional perspective of the pressure distribution in a horizontal plane at $Y/D = 3.46$.

IV. Conclusions

Two numerical procedures have been used together with the two-equation $k - \epsilon$ turbulence model to simulate the flow of a single impinging jet through a confined crossflow for $H/D = 5$ and $V_j/U_0 = 30$. The hybrid central/upwind differencing scheme allows false diffusion errors that prevent grid independence being achieved on reasonable meshes. The use of the quadratic upstream-weighted differencing scheme yields more accurate solutions with coarser meshes. The results presented here are only a sample of those computed in evaluating this method, but illustrate the good agreement with experiments. However, the shear stress distribution in the impingement zone is not predicted correctly due to known shortcomings of the $k - \epsilon$ turbulence model. The calculations obtained with the QUICK differencing scheme show that the maximum height of the ground vortex is about 40% of the jet-exit height and reveal the existence of large low-pressure regions that for a VSTOL aircraft may produce a substantial negative lift.

Acknowledgments

The present work has been performed in collaboration between the "Centro de Termodinâmica Aplicada e Mecânica dos Fluidos da Universidade Técnica de Lisboa," CTAM-FUTL-INIC, and the Fluids Section of the Imperial College of Science and Technology.

References

[1]Keffer, J. F. and Baines, W. D., "The Round Turbulent Jet in a Cross-wind," *Journal of Fluid Mechanics,* Vol. 15, 1963, pp. 481-496.

[2]Adler, D. and Baron, A., "Prediction of a Three-Dimensional Circular Turbulent Jet in Crossflow," *AIAA Journal,* Vol. 17, Feb. 1979, pp. 168-174.

[3]Patankar, S. V., Basu, D. K., and Alpay, S. A., "Prediction of the Three-Dimensional Velocity Field of a Deflected Jet," *Journal of Fluids Engineering,* Vol. 99, Dec. 1977, pp. 758-762.

[4]Ramsey, J. W. and Goldstein, R. J., "Interaction of Heated Jet with a Deflecting Stream," NASA CR-72613, 1972.

[5]Rodi, W. and Srivatsa, S. K., "A Locally Elliptic Procedure for Three-Dimensional Flows and its Application to a Jet in a Cross-Flow," *Computer Methods in Applied Mechanics and Engineering,* Vol. 23, No. 1, July 1980, pp. 67-83.

[6]Baker, A. J., Manhardt, J. A., Orzechowski and Yen, K. T., "A Three-Dimensional Finite Element Algorithm for Prediction of V/STOL Jet-Induced Flowfields," AGARD CP-308, Paper 26, 1982.

[7]Jones, W. P. and McGuirk, J. J., "Computation of a Round Turbulent Jet Discharging into a Confined Crossflow," *Turbulent Shear Flows 2,* edited by L. Bradbury, Springer-Verlag, Berlin, 1980, pp. 233-245.

[8]Demuren, A. O., "Numerical Calculations of Steady Three-Dimensional Turbulent Jets in Crossflow," *Computer Methods in Applied Mechanics and Engineering,* Vol. 37, No. 3, May 1983, pp. 309-328.

[9]Childs, R. E. and Nixon, D., "Simulation of Impinging Turbulent Jets," *Proceedings of the AIAA 23rd Aerospace Sciences Meeting,* AIAA Paper 85-0047, AIAA, New York, 1985.

[10]Barata, J. M. M., Durão, D. F. G., Heitor, M. V., and McGuirk, J. J., "The Turbulence Characteristics of the Single Impinging Jet Through a Crossflow," *Proceedings of the Sixth Symposium on Turbulent Shear Flows,* Toulouse, France, Sept., 1987.

[11]Leonard B. P., "A Stable and Accurate Convective Modelling Procedure Based on Quadratic Upstream Interpolation," *Computer Methods in Applied Mechanics and Engineering,* Vol. 19, No. 1, 1979, pp. 59-98.

[12]Launder, B. E. and Spalding, D. B., "The Numerical Computation of Turbulent Flows," *Computer Methods in Applied Mechanics, and Engineering,* Vol. 3, 1974, pp. 269-289.

[13]Leonard B. P., Leschziner, M. A., and McGuirk, J. J., "Third-Order Finite-Difference Method for Steady Two-Dimensional Convection," *Proceedings of the 1st International Conference on Numerical Methods in Laminar and Tubulent Flow,* edited by C. Taylor et al., Pentech Press, London, 1978.

[14]Gosman, A. D. and Pun. W. M., "Calculation of Recirculating Flows," Imperial College Rept. HTS/74/2, Imperial College, London, 1974.

[15]Han, T., Humphrey, J. A. C., and Launder, B. E., "A Comparison of Hybrid and Quadratic-Upstream Differencing in High Reynolds Number Elliptic Flows," *Computer Methods in Applied Mechanics and Engineering*, Vol. 29, No. 1, Oct. 1981, pp. 81–95.

[16]Rhode, D. L., Demko, J. A., Traegner, U. K., Morrison, G. R., and Sobolik, S. R., "Prediction of Incompressible Flow in Labyrinth Seals," *Journal of Fluids Engineering*, Vol. 108, March 1986, pp. 19–25.

[17]Leschziner, M. A. and Rodi, W., "Calculation of Annular and Twin Parallel Jets Using Various Discretization Schemes and Turbulence Model Variants," *Journal of Fluids Engineering*, Vol. 103, June 1981, pp. 352–360.

[18]Patankar, S. V. and Spalding, D. B., "A Calculation Procedure for Heat, Mass and Momentum Transfer in Three-Dimensional Parabolic Flows," *International Journal of Heat and Mass Transfer*, Vol. 15, Oct. 1972 pp. 1787–1805.

U.S. Postal Service

STATEMENT OF OWNERSHIP, MANAGEMENT AND CIRCULATION

Required by 39 U.S.C. 3685)

1A. Title of Publication	1B. PUBLICATION NO.	2. Date of Filing
Journal of Aircraft	2 7 8 0 8 0	9/28/89
3. Frequency of Issue	3A. No. of Issues Published Annually	3B. Annual Subscription Price
Monthly	12	$26.00

4. Complete Mailing Address of Known Office of Publication *(Street, City, County, State and ZIP+4 Code) (Not printers)*

370 L'Enfant Promenade S.W., Washington, D.C. 20024

5. Complete Mailing Address of the Headquarters of General Business Offices of the Publisher *(Not printer)*

Same as above.

6. Full Names and Complete Mailing Address of Publisher, Editor, and Managing Editor ***(This item MUST NOT be blank)***

Publisher *(Name and Complete Mailing Address)*

American Institute of Aeronautics and Astronautics, Inc. (Same as above.)

Editor *(Name and Complete Mailing Address)*

Thomas M. Weeks -- Same as above.

Managing Editor *(Name and Complete Mailing Address)*

William O'Connor -- Same as above.

7. Owner *(If owned by a corporation, its name and address must be stated and also immediately thereunder the names and addresses of stockholders owning or holding 1 percent or more of total amount of stock. If not owned by a corporation, the names and addresses of the individual owners must be given. If owned by a partnership or other unincorporated firm, its name and address, as well as that of each individual must be given. If the publication is published by a nonprofit organization, its name and address must be stated.) (Item must be completed.)*

Full Name	Complete Mailing Address
American Institute of Aeronautics and Astronautics, Inc.	Same as above.

8. Known Bondholders, Mortgagees, and Other Security Holders Owning or Holding 1 Percent or More of Total Amount of Bonds, Mortgages or Other Securities *(If there are none, so state)*

Full Name	Complete Mailing Address
None.	

9. For Completion by Nonprofit Organizations Authorized To Mail at Special Rates *(DMM Section 423.12 only)*
The purpose, function, and nonprofit status of this organization and the exempt status for Federal income tax purposes *(Check one)*

(1) [X] Has Not Changed During Preceding 12 Months (2) [ ] Has Changed During Preceding 12 Months *(If changed, publisher must submit explanation of change with this statement.)*

10. Extent and Nature of Circulation *(See instructions on reverse side)*	Average No. Copies Each Issue During Preceding 12 Months	Actual No. Copies of Single Issue Published Nearest to Filing Date
A. Total No. Copies *(Net Press Run)*	3,825	3,900
B. Paid and/or Requested Circulation 1. Sales through dealers and carriers, street vendors and counter sales	-----	-----
2. Mail Subscription *(Paid and/or requested)*	3,385	3,492
C. Total Paid and/or Requested Circulation *(Sum or 10B1 and 10B2)*	3,385	3,492
D. Free Distribution by Mail, Carrier or Other Means Samples, Complimentary, and Other Free Copies	156	141
E. Total Distribution *(Sum of C and D)*	3,541	3,633
F. Copies Not Distributed 1. Office use, left over, unaccounted, spoiled after printing	284	267
2. Return from News Agents	-----	-----
G. TOTAL *(Sum of E, F1 and 2—should equal net press run shown in A)*	3,825	3,900

11. I certify that the statements made by me above are correct and complete	Signature and Title of Editor, Publisher, Business Manager, or Owner
	David Quackenbush, Controller

PS Form **3526**, Dec. 1987 *(See instructions on reverse)*